Clim Dyn
DOI 10.1007/s00382-012-1319-y

# A comparative study of the Indian summer monsoon hydroclimate and its variations in three reanalyses

**Vasubandhu Misra · P. Pantina · S. C. Chan · S. DiNapoli**

Received: 21 April 2011 / Accepted: 16 February 2012


**Abstract** This study examines the Indian summer monsoon hydroclimate in the National Centers for Environmental Prediction (NCEP)-Department of Energy (DOE) Reanalysis (R2), the Climate Forecast System Reanalysis (CFSR), and the Modern Era Retrospective-Analysis for Research and Applications (MERRA). The three reanalyses show significant differences in the climatology of evaporation, low-level winds, and precipitable water fields over India. For example, the continental evaporation is significantly less in CFSR compared to R2 and MERRA. Likewise the mean boreal summer 925 hPa westerly winds in the northern Indian Ocean are stronger in R2. Similarly the continental precipitable water in R2 is much less while it is higher and comparable in MERRA and CFSR. Despite these climatological differences between the reanalyses, the climatological evaporative sources for rain events over central India show some qualitative similarities. Major differences however appear when interannual variations of the Indian summer monsoon are analyzed. The anomalous oceanic sources of moisture from the adjacent Bay of Bengal and Arabian Sea play a significant role in determining the wet or dry year of the Indian monsoon in CFSR. However in R2 the local evaporative sources from the continental region play a more significant role. We also find that the interannual variability of the evaporative sources in the break spells of the intraseasonal variations of the Indian monsoon is stronger than in the wet spells. We therefore claim that instead of rainfall, evaporative sources may be a more appropriate metric to observe the relationship between the seasonal monsoon strength and intraseasonal activity. These findings are consistent across the reanalyses and provide a basis to improve the predictability of intraseasonal variability of the Indian monsoon. This study also has a bearing on improving weather prediction for tropical cyclones in that we suggest targeting enhanced observations in the Bay of Bengal (where it is drawing the most moisture from) for improved analysis during active spells of the intraseasonal variability of the Indian monsoon. The analysis suggests that the land–atmosphere interactions contribute significant uncertainty to the Indian monsoon in the reanalyses, which is consistent with the fact that most of the global reanalyses do not assimilate any land-surface data because the data are not available. Therefore, the land–atmosphere interaction in the reanalyses is highly dependent on the land-surface model and it's coupling with the atmospheric model.

This paper is a contribution to the special issue onGlobal Monsoon Climate, a product of the Global Monsoon WorkingGroup of the Past Global Changes (PAGES) project, coordinated byPinxian Wang, Bin Wang, and Thorsten Kiefer.

V. Misra (✉)
Department of Earth, Ocean and Atmospheric Science, Florida State University, Tallahassee, FL, USA
e-mail: vmisra@fsu.edu

V. Misra · S. DiNapoli
Center for Ocean-Atmospheric Prediction Studies, Florida State University, Tallahassee, FL, USA

P. Pantina
Science Systems and Application, Inc., 10210 Greenbelt Road, Ste. 600, Lanham, MD 20706, USA

P. Pantina
Cloud and Radiation Laboratory, NASA/GSFC, Greenbelt, MD, USA

S. C. Chan
School of Civil Engineering and Geosciences, Newcastle University, Newcastle upon Tyne, UK

S. C. Chan
Met Office Hadley Center, Exeter, UK
e-mail: steven.chan@metoffice.gov.uk

Published online: 08 March 2012

**Keywords** Monsoon · Intraseasonal · Interannual

## 1 Introduction

The Indian monsoon is a boreal summertime (June–September) phenomenon that coincides with an annual reversal of the winds over India and the occurrence of 75–90% of the country's annual precipitation (Mooley and Parthasarathy 1984). Indian agricultural success is highly dependent on precipitation since crops are largely rain fed across most of the country (Kerr 1996). Moisture source studies are necessary for improved understanding and prediction of the seasonal characteristics of the monsoon.

From the earlier works of Delworth and Manabe (1988, 1989) to the more recent work of Koster et al. (2004), there has been a realization that the soil moisture anomaly impacts the seasonal and interannual variability of "drier" Indian and northeast Asian monsoons more considerably than it impacts the southeast Asian monsoon. These results allude to the fact that in the former monsoon regions, the evaporation is more moisture limited, whereas in the latter, it is more energy limited. Similar conclusions are also drawn from a more recent global modeling study by Misra (2008). In a moisture-limited regime, evaporation is limited by the soil moisture availability, while in an energy limited regime, evaporation is limited by net radiative energy at surface.

Moisture sources are not limited to local evaporation processes; advection of moisture from nearby landmasses or from ocean basins by winds is equally important in contributing to moisture for precipitation. Brubaker et al. (1993) and Benton et al. (1950) concluded that water vapor from the oceans could pass over continental regions without immediately raining out as precipitation. Budyko (1974) concluded that most of the precipitation is generated from moisture of "external origin" rather than of local origin. Evaporation off the oceans is a large component here, as moisture is unlimited (Trenberth et al. 1999). However, remote land regions also contribute to externally originating moisture, as upstream evaporation over the surface creates atmospheric moisture that may be advected by winds (Brubaker et al. 1993). Trenberth and Guillemot (1998) claimed that this terrestrial- and marine-based atmospheric moisture either flows past a region or converges over it and precipitates out; the mechanism depends on the dynamics of the circulation.

Remote advection of moisture also plays an important role in the Indian summer monsoon. Cadet and Reverdin (1981) showed that the onset of the Indian monsoon is associated with cross-equatorial water vapor transport passing from eastern Africa, over the Arabian Sea, and into India. In this study, we subsequently refer to this area as the "monsoon flow region." Cadet and Reverdin concluded that 70% of the moisture passing over the southwestern coast of India originates from the Southern Hemisphere and that the remaining moisture advects in from the Arabian Sea along the path of the flow. Likewise, Lim et al. (2002) isolated two main regions of moisture over southern Asia in their study of the seasonal cycle of the Asian monsoon. They showed that a continuous supply of moisture from the Indian Ocean, as well as from the western Pacific Ocean, sustains the seasonal monsoon rainfall events that occur during the boreal summer. The present study will intercompare the reanalyses in the depiction of the evaporative sources and their variability for rain events in central India, which is considered the main region of the mean Indian summer monsoon (Krishnamurthy and Shukla 2000, 2006; Goswami and Ajayamohan 2001).

Evaporative source is defined as the origin of water molecules for precipitation over a region (Dirmeyer and Brubaker 1999). The sources of precipitation originate from moisture already in the atmosphere over the region, from the convergence of atmospheric moisture advected into the region by winds, and from evaporation of surface moisture into the atmosphere over the region, either from land or from water (Trenberth et al. 1999). Trenberth et al. (2003) concluded that the largest contributors to rainfall are evaporation and remote advection of moisture.

Evaporative sources can be estimated by using observed precipitation and reanalysis temperature, winds, evaporation, and precipitable water. Using a back-trajectory program, we can trace parcels back in time and isolate uncertainties in the evaporative sources across various available reanalyses, which is the major goal of this study.

The Indian monsoon undergoes substantial interannual variability that we can isolate in the seasonal evaporative sources as well. Using empirical orthogonal function (EOF) analysis, Krishnamurthy and Shukla (2000) demonstrated that drought or flood years are characterized by rainfall anomalies of the same sign over most of the Indian region. Therefore, wet years feature a countrywide increase in rainfall over the monsoon season, whereas dry years feature a countrywide reduction in rainfall. Additionally, the interannual variation of rainfall over India is nonperiodic, such that dry years do not immediately precede or follow wet years (Krishnamurthy and Kinter 2003).

Several mechanisms have been proposed to explain monsoon interannual variability. These include the El Niño Southern Oscillation (Kumar et al. 1999; Krishnamurthy and Kinter 2003; Kirtman and Shukla 2000), the tropical biennial oscillation (TBO) (Meehl 1994, 1997), the snow cover over western Eurasia (Bamzai and Shukla 1999), and the Indian Ocean dipole (Saji et al. 1999; Krishnamurthy and Kirtman 2003, 2009). Overall, these mechanisms feature large-scale changes in monsoon circulation and

incorporate either land-sea temperature contrasts or shifts in the tropical Walker circulation to explain changes in rainfall. Wang et al. (2001) suggested that monsoon interannual variability is generally dictated by these large-scale alternations in atmospheric patterns, and noted a strengthening of the entire monsoon circulation, including the monsoon trough and the low-level cross equatorial flow, during above-average monsoon seasons.

Intraseasonal variability is a significant component of Indian monsoon variability. Krishnamurthy and Shukla (2000) used EOF analysis to isolate the major mode of intraseasonal variation and found that anomalies of one sign exist over most of central India and that opposite-signed anomalies exist over the northern plains and far western India.

Krishnamurthy and Shukla (2006) attributed some of the Intra-Seasonal Oscillation (ISO) activity to the passage of low pressure systems (LPSs) over India from the Bay of Bengal. During active periods, the number of days when a LPS is recorded in the Indian monsoon region increases dramatically, up to seven times that of a break period (Krishnamurthy and Shukla 2006).

There has been substantial debate regarding the existence of interannual variability of the monsoon ISOs. Goswami and Ajayamohan (2001) suggested a higher occurrence of active (break) periods during a strong (weak) monsoon. They concluded that the probability density functions (PDFs) of ISO activity are asymmetric and different in wet and dry years. Lawrence and Webster (2001) argued that ISO activity is inversely correlated to the seasonal Indian monsoon rainfall activity. They showed that when ISO activity is strong during the summer (i.e., several active and break periods in a given season), seasonal monsoon strength is weak. However, Singh et al. (1992) concluded that there is no relationship between ISO activity and seasonal mean monsoon rainfall. Similarly, Jones et al. (2004) found that there is no statistically significant difference in tropical intraseasonal activity from year to year. In this study, we will attempt to isolate interannual variability of the evaporative sources for intraseasonal rainfall events over central India to further understand the interannual variations of the ISO.

In Sect. 2 we provide details of the rainfall and reanalysis datasets used in the study, and we discuss potential problems with the reanalysis parameters. In Sect. 3, we outline the methods used to isolate interannual and intraseasonal variability, and we describe the quasi-isentropic back trajectory program that we used to trace moisture sources. We analyze the results of the study in Sect. 4. We break the results into four separate parts; (1) seasonal climatology of reanalysis parameters; (2) interannual variability of reanalysis parameters; (3) seasonal climatology and interannual variability of evaporative sources; and (4) intraseasonal variability of evaporative sources. We provide a discussion of the results and concluding remarks in Sect. 5.

## 2 Data

### 2.1 Rainfall

This study incorporates the Indian Meteorological Department (IMD) high–resolution daily gridded rainfall dataset over the Indian region (Rajeevan et al. 2006). The IMD rain-gauge-based dataset is interpolated to a 1°latitude × 1°longitude grid over India and spans each day for the period 1951–2003. The data are interpolated using a weighted-sum method with radii of influence developed by Shepard (1968). The grid covers the entire country and surrounding waters, but has values of rainfall only over land.

We also incorporate the satellite-based Climate Prediction Center (CPC) morphing method (CMORPH) precipitation estimates (Joyce et al. 2004). These are global precipitation analyses that are available on a high-resolution (eight-square-kilometer) grid. They are derived from passive satellite microwave scans as well as geostationary satellite infrared (IR) scans. The morphing technique uses motion vectors derived half-hourly from the IR data to advect the precipitation estimates received from the passive microwave data. CMORPH is used to correct the diurnal cycle of precipitation in the different reanalyses at tropical latitudes according to Dirmeyer and Brubaker (1999).

### 2.2 Reanalysis

This study uses three different reanalysis products. These include the National Centers for Environmental Prediction/Department of Energy (NCEP/DOE) Reanalysis-2 (also referred to as R2; Kanamitsu et al. 2002), the NCEP Climate Forecast System Reanalysis (CFSR; Saha et al. 2010), and the Modern Era Retrospective-Analysis for Research and Applications (MERRA; Bosilovich et al. 2008; Rienecker et al. 2011) datasets. The variables used from this reanalysis are surface latent heat flux (evaporation), surface precipitation rate, surface pressure, specific humidity, temperature, and the zonal and meridional components of the wind. Potential temperature and precipitable water (PW) are calculated from surface pressure and temperature, and from specific humidity, respectively.

First, we make use of the six-hourly global T62 Gaussian-gridded (192 × 81) R2 upper-air data available at 17 pressure levels along with the land surface data. The data are available from 1979 to the present. R2 uses a two-layer land surface model (LSM) developed at Oregon State University (OSU; Pan and Mahrt 1987). It estimates the movement of water between a thin upper layer, which responds to diurnal changes in weather, and a thicker lower layer, which responds to changes in climate. The OSU scheme has essentially two soil layers, which are 10 and 190 cm thick. The soil moisture and temperature are

predicted in these two layers in addition to water content in the canopy. The surface skin temperature is diagnosed from the surface energy balance. The soil temperature is predicted using the diffusion equation with the skin temperature as top boundary condition and anomaly averaged climatological deep soil temperature for bottom boundary condition. The soil hydrology is solved using the Richardson's equation. The transpiration is a function of soil layer thickness, vegetation fraction, potential evaporation, canopy resistance and canopy water content (Ek and Mahrt 1991).

We also make use of six-hourly global T382 Gaussian-gridded (1152 × 576) CFSR upper-air data available on 17 pressure levels with the associated land surface data. The data are available from 1979 to the present day. This dataset was completed in January 2010 and uses a coupled atmosphere–ocean-land surface-sea ice system (Saha et al. 2010). The CFSR uses the Noah LSM (Ek et 2003). In comparison to the OSU scheme used in R2, Noah has 4 soil layers (10, 30, 60 and 100 cms thick) with root zone depth spatially varying as a function of vegetation class. The frozen soil physics and snow pack has undergone refinements in the Noah (Koren et al. 1999). Likewise improvements have also been made to ground heat flux, canopy conductance, surface runoff, infiltration, and soil thermal conductivity (Ek et al. 2003). For example the catastrophic shutting of evaporation as soil moisture begins to dry in the OSU scheme is now made to gradually reduce with decreasing soil moisture (Betts et al. 1997). Similarly the transpiration refinements adopted through changes in the canopy conductance in Noah has improved the ability to recharge the soil moisture during wet periods and discharge it during dry periods. Overall Noah LSM is found to improve the simulation of the surface meteorology relative to the OSU scheme (Ek et al 2003; Robock et al. 2003; Mitchell et al. 2004).

Finally, we use six-hourly global (540 × 361), Gaussian-gridded MERRA upper-air (on 42 pressure levels) and one-hourly global (540 × 361), Gaussian-gridded MERRA land surface data. The data are a NASA-based product and are available from 1979 to 2007. The data assimilation model of MERRA uses NASA's Catchment based LSM (CLSM; Koster et al. 2000), which, like the Noah-LSM, dynamically predicts land surface water and energy fluxes. However, it uses a topographically based approach instead of a layer-based approach to soil moisture. The CLSM uses topographic characteristics and bulk moisture variables to predict soil moisture for each catchment, or computation unit, of the model. It then calculates the distribution of moisture at a sub-catchment level, which is considered an improvement over traditional one-dimension LSMs such as the Noah-LSM. However, Kumar et al. (2008) concluded that both the Noah-LSM and the CLSM exhibit soil moisture that responds similarly to forcing from the atmosphere and yield comparable values for that field.

Table 1 summarizes some of the main differences between the reanalysis. From the table it should also be noted that besides using different assimilation models in the three reanalyses, they also adopt different data assimilation procedures. Furthermore, although the conventional observations used in the three analyses are similar, the predominance of satellite based observations in the recent decades and the ability to directly assimilate radiances in CFSR and MERRA are other major advances from R2.

### 2.3 Problems with reanalysis estimates

Model-based estimates, such as surface evaporation rate or latent heat flux, should be viewed with caution. Evaporation is "amongst the most poorly measured hydroclimate fields" (Nigam and Ruiz-Barradas 2006), but it plays an important role in the water balance and evaporative sources of the Earth system as explained above. Since it cannot be directly measured, evaporation is estimated, sometimes

**Table 1** A brief comparison of the reanalyses

| Feature | R2 | CFSR | MERRA |
|---|---|---|---|
| Horizontal grid resolution | ~200 km | ~38 km | ~55 km |
| Vertical resolution | 28 terrain following $\sigma$ levels with top pressure 3 hPa | 64 terrain following $\sigma$ levels with top pressure ~0.266 hPa | 72 generalized vertical co-ordinates with top pressure ~0.01 hPa |
| Atmospheric data assimilation model | Kanamitsu et al. (2002) | Saha et al. (2010) | Rienecker et al. (2011) |
| Land surface model | OSU (Pan and Mahrt 1987) | Noah (Ek et al. 2003) | Catchment based (Koster et al. 2000) |
| SST | Prescribed from Reynolds weekly 1° SST v2 (Reynolds et al. 2002) | Obtained from coupled GFDL MOM version 4 | Prescribed from the weekly 1° SST following Reynolds et al. (2002) |
| Assimilation methodology | Spectral statistical interpolation (Parrish and Derber 1992; Derber et al. 1991) | Gridpoint statistical interpolation (GSI; Kleist et al. 2009) and using coupled 6-hour forecast for first guess field (Saha et al. 2010) | GSI with incremental analysis update (Bloom et al. 1996) |

inaccurately, from reanalysis land surface models that are driven by observed parameters such as precipitation and temperature (Ruiz-Barradas and Nigam 2004). The reanalysis land surface models tend to be unreliable because of poor model physics, varied resolution, and sparse observations. Since each of the three reanalyses we use in this study has its own land surface model, it is clear that the prominent uncertainties in the moisture sources we wish to track will most likely stem from uncertainty in evaporation between reanalyses.

## 3 Methodology

### 3.1 Isolating interannual variability

Rainfall data from the IMD gridded dataset are area-averaged over all-India from 1 June to 30 September for each year from 1951 to 2003. The five wettest and driest years after 1979 are selected and labeled as wet and dry, respectively. We also include 5 years with small (within 3% of normal) deviation from the climatological mean and label them as neutral; these years are included to increase our sample size and give a basis for average conditions. The years are listed in Table 2, along with each year's seasonal rainfall deviation from the long-term mean.

### 3.2 Isolating intraseasonal variability

Rainfall anomaly data from the IMD are area-averaged over central India (73°E–86°E and 16°N–26°N) for each day (15 May–15 October) for each year of interest to create a 154- day time series. We then extract the low-frequency 20-60-day mode from this time series using a recursive first-order Butterworth filter (Krishnamurti and Subrahmanyam 1995). We record an active (break) period if a continuous string of 10–30 days is above (below) zero in this filtered time series. We compare the intraseasonal oscillations isolated from the Butterworth filter with the raw time series after the seasonal mean is removed (not shown). For most years, the general trends in increasing and decreasing rainfall throughout the season are well captured by the filtered oscillations.

### 3.3 Quasi-isentropic back trajectory program

We use a quasi-isentropic back trajectory (QIBT) program to isolate the evaporative sources of precipitation events over central India. Dirmeyer and Brubaker (1999) developed this method for a similar study of evaporative source variability over the central United States. We trace the evaporative sources for central India rainfall events because they are a good representation of the all-India monsoon rainfall anomalies (Gadgil 2003; Krishnamurthy and Shukla 2000). We give a basic description of the program's mechanisms in the following section but refer readers to Dirmeyer and Brubaker (1999) for complete details.

Following the technique of Dirmeyer and Brubaker (1999), we first release one hundred saturated air parcels at a random humidity-weighted interval at every grid point where and when rain has fallen over central India (73°E–86°E and 16°N–26°N). The moisture content of the parcels is equal to the amount of rainfall at the initial grid point summed over the pentad, or five-day period, under consideration. Summertime (JJAS) pentads range from 30 to 55 (26 May–2 October). Each parcel is tagged with the environmental potential temperature (calculated from surface pressure and temperature) and isentropically (on constant potential temperature surface) advected backward in time with reanalysis winds. Following Merrill (1989) and Dirmeyer and Brubaker (1999) the parcel trajectory is the average of forward and backward trajectories:

1. A backward trajectory locates a parcel from its original point ($x^n$, $y^n$) at time n to a new point ($x^{n-1*}$, $y^{n-1*}$) at time n − 1* using the winds at time n.
2. A forward trajectory locates a parcel from point ($x^{n-1*}$, $y^{n-1*}$) to another point ($x^{n*}$, $y^{n*}$) back to time n using the winds at time n − 1.

**Table 2** Graph showing each year's deviation from climatological (1951–2003) average of seasonal (JJAS) rainfall over all-India

| Year cases selected from IMD gridded rainfall | | | | | |
|---|---|---|---|---|---|
| Wet years | % Above normal | Dry years | % Above normal | Neutral years | % Above normal |
| 1988 | 14.9 | 2002 | −18.5 | 1996 | −0.0 |
| 1983 | 10.8 | 1979 | −17.9 | 1984 | −0.4 |
| 1998 | 9.9 | 1987 | −12.9 | 1997 | −2.5 |
| 1990 | 8.1 | 1982 | −11.5 | 1989 | 2.9 |
| 1994 | 7.4 | 1986 | −11.3 | 1985 | 3.0 |

The abscissa is the year (note: not sequential) and the ordinate is the percentage difference between a given year's rainfall and the climatological average. Dry years are colored in red, neutral in yellow, and wet in green. The long-term mean is shown by the black solid line and one standard deviation by dashed lines

The backward trajectory and the negative forward trajectory are averaged to arrive at the final point ($x^{n-1}$, $y^{n-1}$), which is then bilinearly interpolated to the nearest grid point. The remote grid point potential temperature is re-evaluated and the parcel is assigned a level in the vertical corresponding to its potential temperature. However if the level of the potential temperature is found to be below the surface then it is assigned the value at the surface so that it never intersects the ground. The time step is hourly; our reanalysis dataset is linearly interpolated from six-hourly to one-hourly. The IMD daily rainfall dataset is interpolated from six-hourly to three-hourly using CMORPH as described by Dirmeyer and Brubaker (1999).

At every time step, we assume that some of the water vapor in a parcel, $k$, comes from the evaporation ($E$) of moisture occurring at the remote grid point ($x$, $y$) directly below it. We then remove water vapor from the parcel at a rate given by:

$$S_{x,y,k,p}(i,j,t) = \frac{E(x,y,p)}{PW(x,y,p)}$$

where $S_{x,y,k,p}(i, j, t)$ represents the source of moisture for initial grid point ($i$, $j$) at pentad time $t$ contributed by evaporation from remote point ($x$, $y$) into parcel $k$ at time step $p$. The back tracing continues for a period of 15 days or until the parcel has lost 90% of its moisture because of the moisture removal dictated by $S_{x,y,k,p}(i,j,t)$. We choose to trace the parcels up to 15 days prior to release to conserve moisture for the individual precipitation events. We observe that the spatial distribution of evaporative source is largely established in the first 5 days (not shown) with minor differences from evaporative sources traced 10, 15, and 20 days back. Therefore we make a conservative choice of tracing evaporative sources back to 15 days.

We can predict the character of the evaporative sources on the basis of the reanalysis parameters alone. The rate of removal fraction in the QIBT indicates that remote evaporation and precipitable water values as well as local rainfall values will have large implications on the length of the back trajectories. High evaporation rates and low values of precipitable water lead to a large moisture removal rate from the parcels, which will remain localized and fail to trace as far back as parcels passing through environments with low evaporation and high precipitable water. Likewise, at initial grid points where rainfall values are high, the parcels have the potential to trace further back in time because they contain more moisture that must originate from the environment. Furthermore, reanalysis winds largely dictate the spatial patterns of the trajectories.

We record the evaporative source of the released parcels every pentad throughout the summer for each reanalysis. To calculate total evaporative source for rainfall at a given grid point ($i$, $j$) at pentad time $t$, we take the sum of individual $S_{x,y,k,p}$ ($i$, $j$, $t$) fields from all global grid points ($x$, $y$), from all parcels, $k$, and through the time of the longest trajectory, $p_f$, to get the contribution of evaporation ($E$) to rainfall over grid point ($i$, $j$) in central India:

$$E(i,j,t) - \sum_{x,y} \sum_{k=1}^{m} \sum_{p=0}^{p_f} S_{x,y,k,p}(i,j,t)$$

We also calculate each reanalysis's recycling ratios, which are the fraction of rainfall that originates from local evapotranspiration to the total rainfall over the region. This ratio ($R$) is given by

$$R = \frac{\sum_{i,j,t} E_A(i,j,t)}{\sum_{i,j,t} P(i,j,t)}$$

where $E_A(i, j, t)$ is the evaporative source totaled over an area A (central India):

$$E_A(i,j,t) = \sum_{A} \sum_{k=1}^{m} \sum_{p=0}^{p_f} S_{x,y,k,p}(i,j,t)$$

There are potential problems with the technique outlined above. Dirmeyer and Brubaker (1999) showed that there are no precipitation sinks incorporated into the trajectory. In other words, the technique does not consider changes to potential temperature due to diabatic processes such as the phase change of water. Chan and Misra (2009) suggested that in many instances this assumption will tend to overextend the trajectories.

## 4 Results

### 4.1 Seasonal climatology of the reanalysis variables

Our QIBT program uses several variables from the three reanalysis datasets to locate sources of moisture for monsoon rainfall events. The variables of most interest to this study are latent heat flux, low-level (925-hPa) winds, and precipitable water (PW). Latent heat flux (evaporation) and PW are related to the rate of removal of moisture from each of our parcels, whereas the winds advect our parcels backward and forward in time. We first analyze the variables from each reanalysis as a seasonal (JJAS) mean.

We calculate simple and percentage differences between various comparisons throughout this study. The percentage difference between field $A$ and field $B$ in this study is given by: $D - 100 \times \frac{A-B}{B}$, where $A$ and $B$ are the fields of the same variables but from different reanalysis or different time frames. The percentage difference $D$ gives the magnitude of the difference between fields $A$ and $B$ in relation to the reference field $B$.

We observe that the seasonal evaporation fields are qualitatively similar across the three datasets (Fig. 1a–c).

Each reanalysis shows large evaporation rates over the water south of India and small evaporation rates over the desert and mountainous regions to the north. In each case, the evaporation is greater over southeastern India than it is over northwestern India, and it decreases as one moves south to north and east to west across India.

We also observe the uncertainty in the evaporation field from each reanalysis by computing its percentage difference from the average analysis. The average analysis is the average of the three reanalyses. We will similarly analyze the uncertainties in wind, PW, and evaporative source between reanalyses.

R2 shows significantly high rates of evaporation over northwestern and southern India, northeastern Pakistan, and portions of central eastern Africa (Fig. 1d). CFSR shows significantly less evaporation over central eastern Africa and India and significantly high evaporation over the Arabian Sea and portions of the Bay of Bengal (Fig. 1e). MERRA reduces evaporation substantially in the Indian Ocean (relative to CFSR) while enhancing over central India (Fig. 1f). Table 3 shows quantitatively that over central India, the climatological summer evaporation is highest in MERRA followed by that in R2 with significantly less evaporation in CFSR (by as much as 15% less than in MERRA). Overall, these comparisons suggest that in boreal summer season, the reanalyses differ qualitatively and quantitatively in their evaporation estimates. Most noticeably, at a seasonal time scale, we observe that CFSR

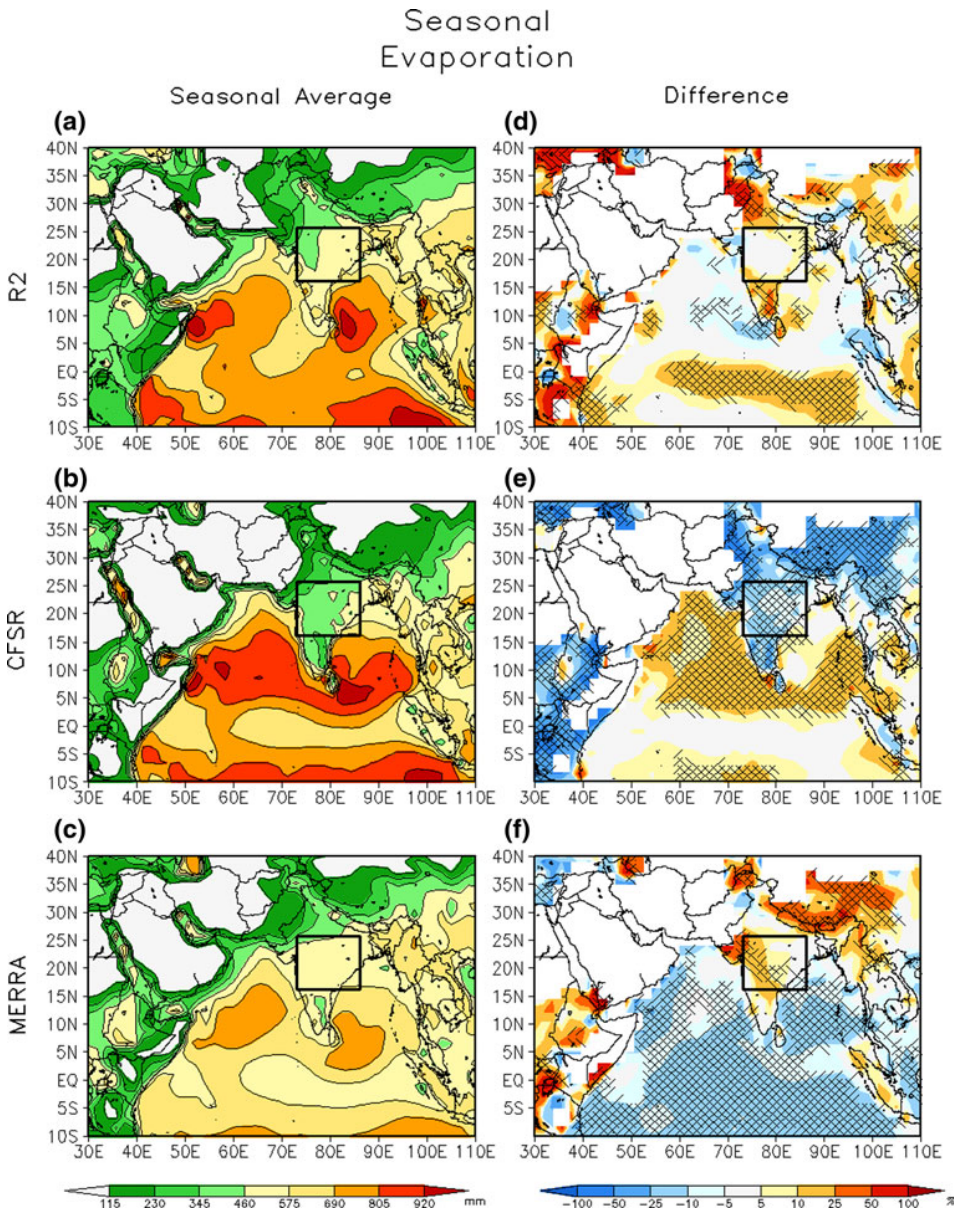


**Fig. 1** Plot showing the seasonal (JJAS) average evaporation rate for the three reanalyses: R2 (**a**), CFSR (**b**), and MERRA (**c**), as well as percentage difference in anomalies between each reanalysis and an average analysis (**d**–**f**). The "average" analysis, the average of each of the three reanalyses evaporation fields, allows consistent comparisons between them. In plotting percentage differences, regions of small evaporation rate are masked so that the differences do not artificially increase in magnitude due to division by small numbers. Areas that are 90% significant are hatched

has significantly reduced continental evaporation compared to the other two reanalyses.

We also analyze average seasonal 925-hPa winds (Fig. 2a–c). The differences indicate that the cross-equatorial and southwesterly monsoon flow is comparatively strongest in R2 (Fig. 2d) and weakest in CFSR (Fig. 2e).

PW fields (Fig. 3a–c) look similar to the fields of evaporation we observed earlier, where PW is highest over

**Table 3** Quantitative estimates of evaporation and precipitable water over central India

| | Evaporation (mm day$^{-1}$) | | | Precipitable water (mm) | | |
|---|---|---|---|---|---|---|
| | R2 | CFSR | MERRA | R2 | CFSR | MERRA |
| All years | 4.10 | 3.58 | 4.22 | 47.46 | 52.77 | 52.41 |
| Dry years | 4.01 | 3.37 | 4.16 | 46.01 | 49.91 | 51.16 |
| Wet years | 4.21 | 3.79 | 4.27 | 49.01 | 55.77 | 52.98 |

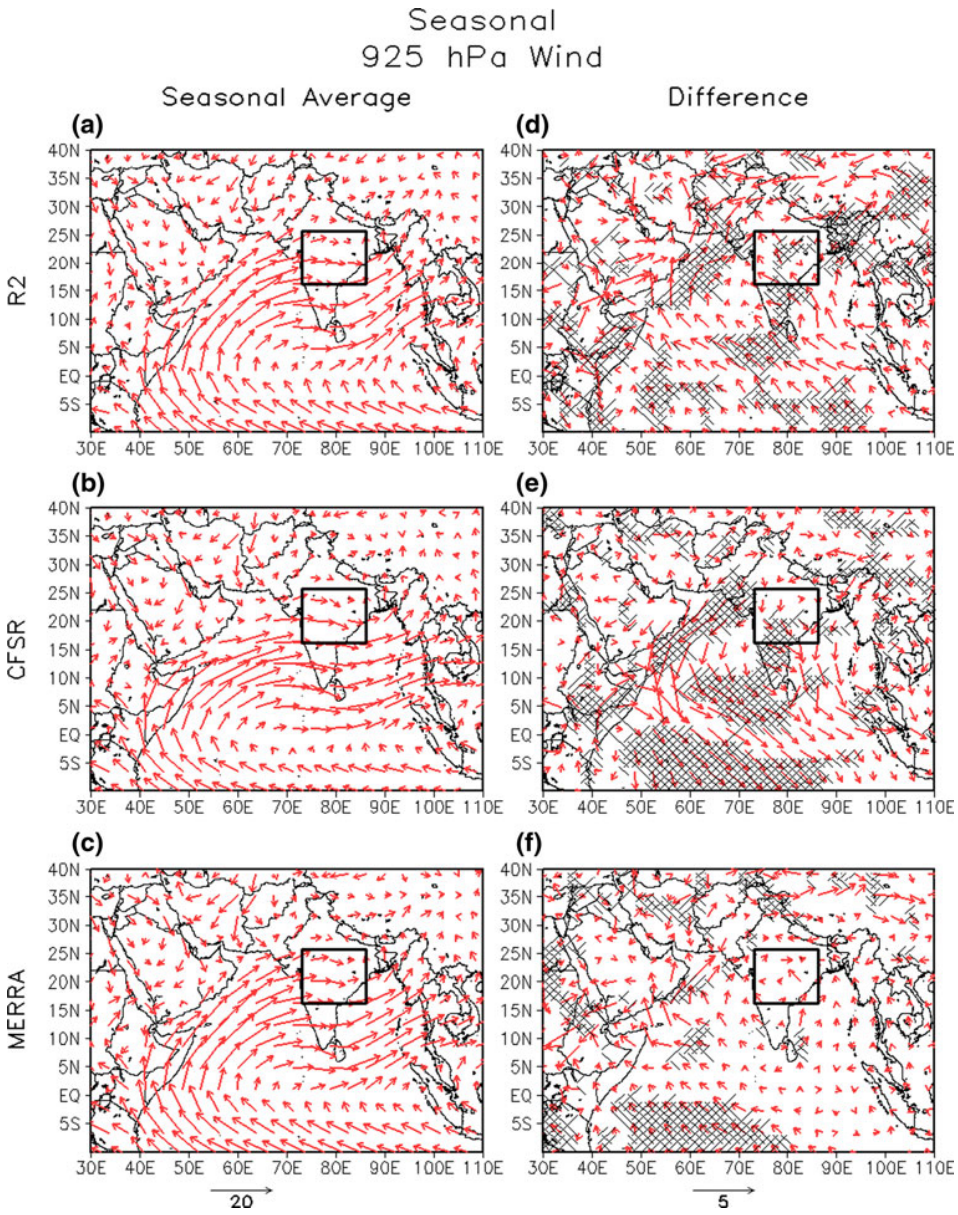


**Fig. 2** Same as Fig. 1, but with 925-hPa winds. The differences here are simple differences and not percentage differences (**d–f**)

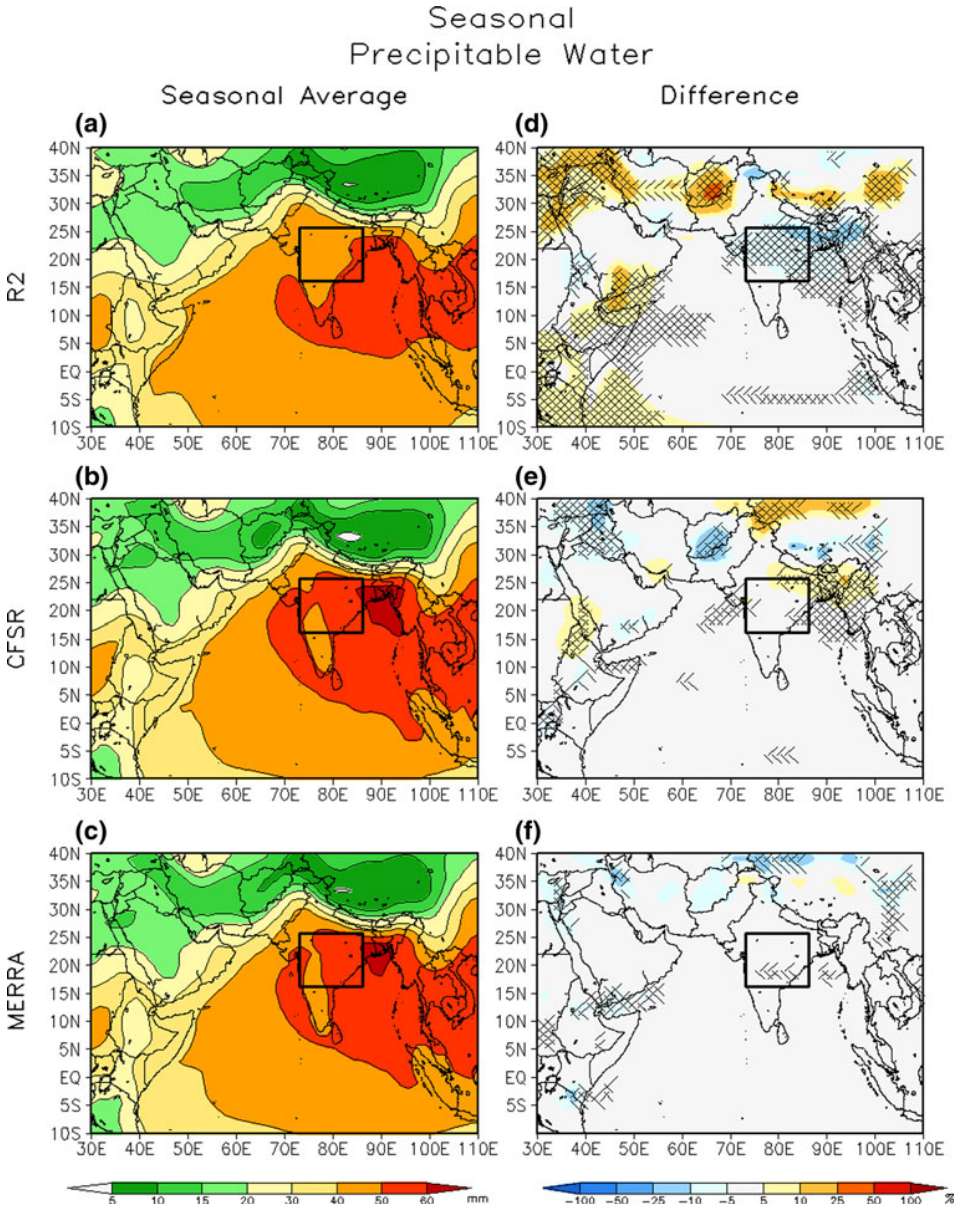


**Fig. 3** Same as Fig. 1, but with PW

the Bay of Bengal and reduces toward the north and west across all reanalyses. When we observe the differences in PW in each reanalysis compared to the average analysis (Fig. 3d–f), we see that R2 features the driest column over India and a slightly wetter column over eastern Africa and southern Arabian Peninsula. The differences shown in Fig. 3e and f indicate that CFSR and MERRA are relatively close to the average analysis. This is also clearly noticed in Table 3, which indicates that the climatological summer PW over central India are nearly comparable in CFSR and MERRA, while it is $\sim$10% less in R2.

### 4.2 Interannual variability of the reanalysis variables

The interannual anomalies of each reanalysis is diagnosed from its own climatology to remove the previously discussed reanalysis bias. The largest differences in interannual variation of evaporation over central India occur in CFSR (Table 3; Fig. 4b and e) followed by that in R2 (Table 3; Fig. 4a, d). The interannual variability of evaporation in MERRA over central India is relatively weaker (Table 3; Fig. 4c and f). Interestingly, the northern Indian Ocean evaporation fields display relatively little interannual variability in the reanalyses.

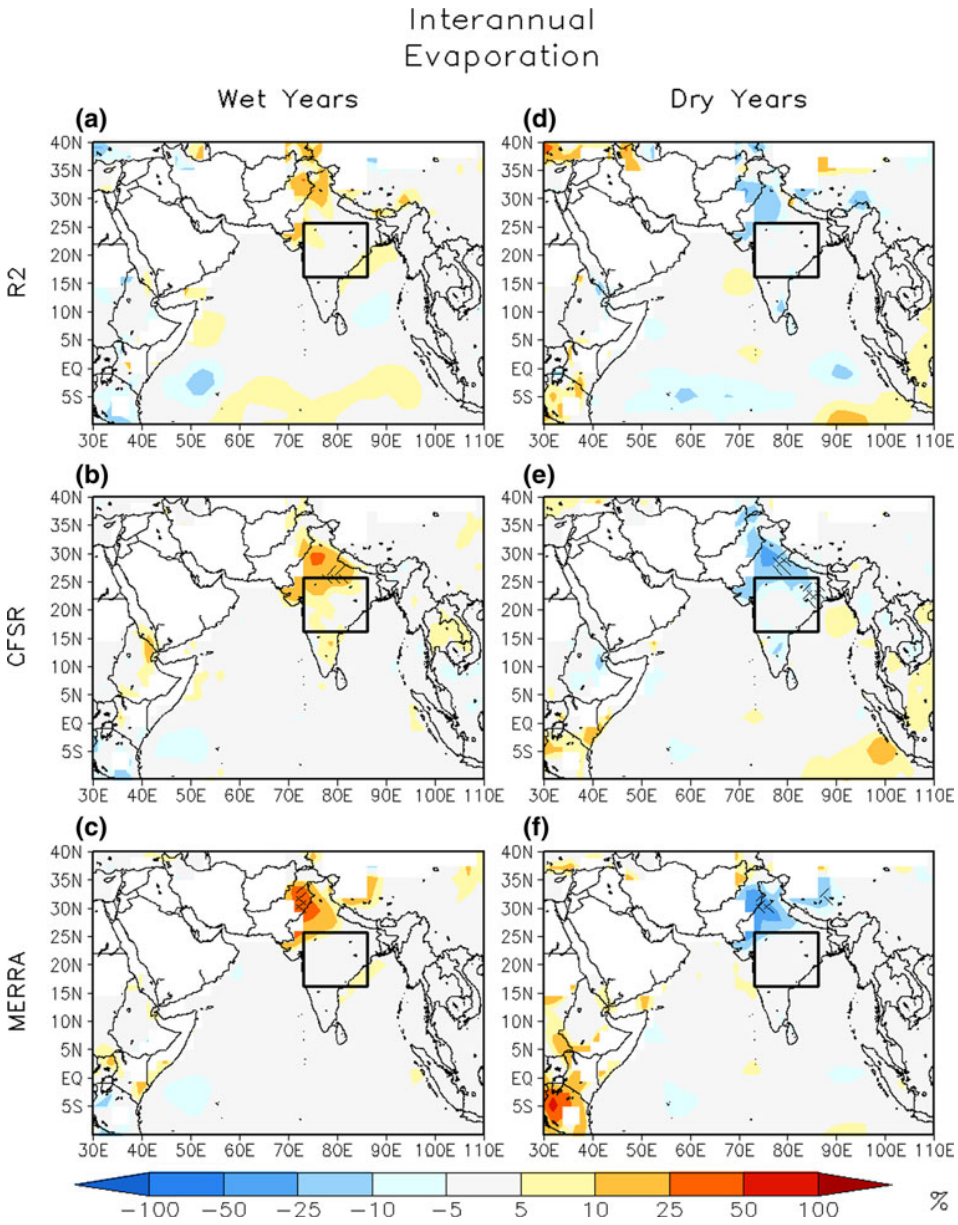


**Fig. 4** Plots showing the percentage differences in evaporation between wet years and climatology for R2 (**a**), CFSR (**b**), and MERRA (**c**). The climatology is computed separately for each reanalyses. Plots **d**–**f** show the same for dry years

The year-to-year variations in the 925-hPa winds are also noticeable. We observe a strengthening in the westerlies over the Arabian Sea and in the monsoon trough (Fig. 5a–c) during wet years. Likewise, there is a reduction in the westerlies and southwesterlies in all reanalyses (Fig. 5d–f) during dry years.

Figure 6 shows the percentage difference in PW between wet and dry monsoon years for each reanalysis. All three reanalyses uniformly show over northern India there is a general increase (decrease) in the moisture column during wet (dry) years. Table 3 also indicates that CFSR displays the strongest interannual variation of PW over central India (with nearly 11% difference between wet and dry years) followed by that in R2 ($\sim$6%), with least in MERRA ($\sim$4%).

### 4.3 Evaporative sources: seasonal climatology and interannual variability

We now examine the seasonal evaporative sources and their uncertainties (or differences across reanalyses) for rain events in central India. Figure 7a–c show the seasonal climatology of the evaporative source from the three reanalyses. These plots seem to indicate that evaporative sources are similar between the reanalysis with significant fraction of contribution of local continental origin.

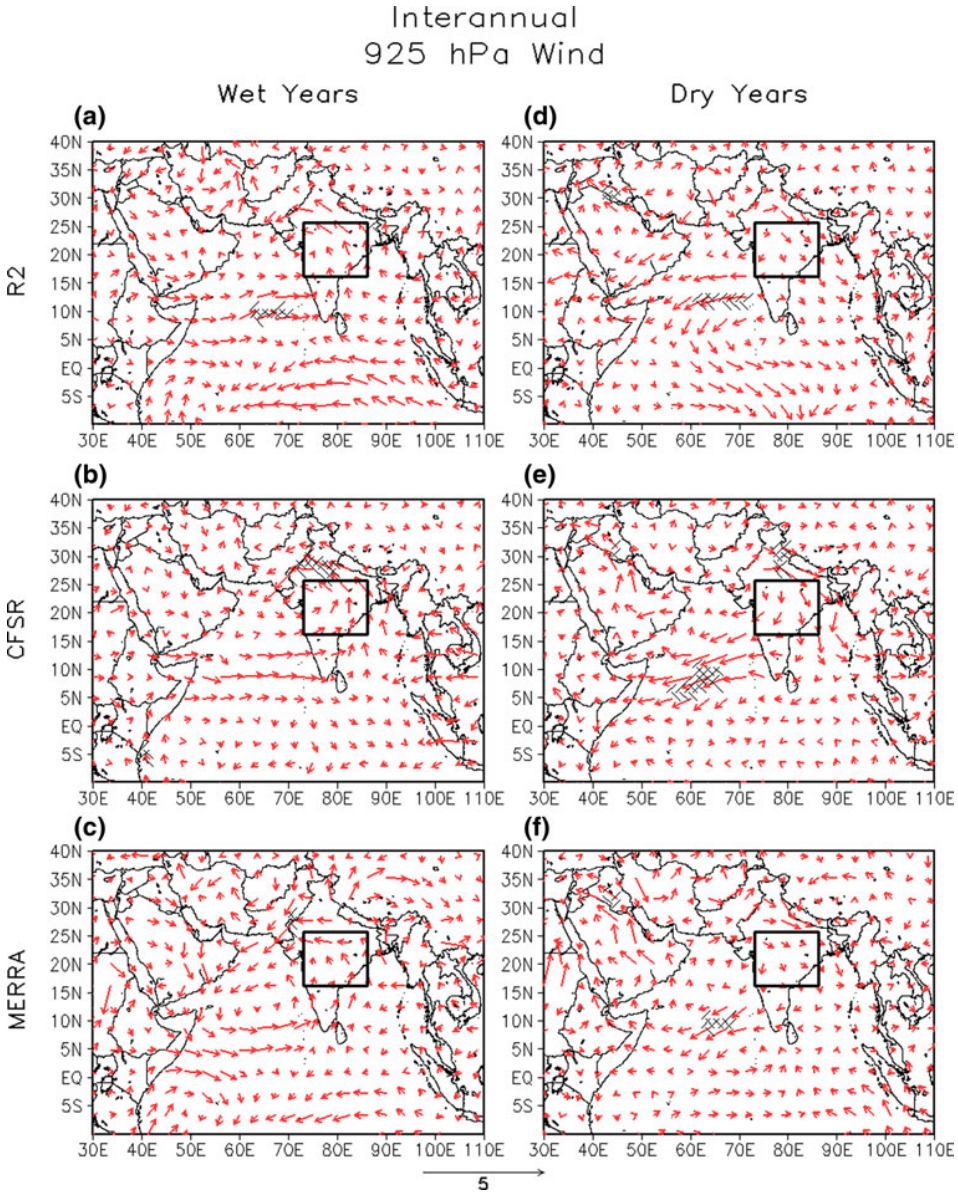


**Fig. 5** Same as Fig. 4, but for 925-hPa winds. Simple differences are shown here

However, the percentage differences (Fig. 7d–f) clearly show that in R2, the largest evaporative sources for central India rain events originate from the northwestern parts of the sub-continent and the coastal oceans of east Africa while underestimating in the neighboring Arabian Sea and Bay of Bengal. On the other hand, CFSR emphasizes the oceanic evaporative sources from the Arabian Sea, the Bay of Bengal, and the South China Sea. The evaporative source in MERRA is relatively close to the average analysis and does not feature significant contribution of moisture from any one specific region.

As anticipated, remote sources are favored in CFSR (oceanic moisture) and local sources are favored in R2 (northwestern India and Pakistan). We attribute this regime to the fact that evaporation is locally high in R2 while it is locally low in CFSR. Furthermore, another contributing factor for the differences in the evaporative sources of the rain events in central India is that the PW in the vicinity of central India is much lower in R2 than in CFSR. Although winds are generally stronger in R2 than they are in CFSR (Fig. 2), which would imply stronger influence of remote moisture in R2, the results indicate that the local evaporation and PW have a dominating role here. MERRA enhances the oceanic evaporative source while reducing the local evaporative source relative to R2 primarily from more moist atmospheric column. But these differences in evaporative sources are far less than those depicted by CFSR.

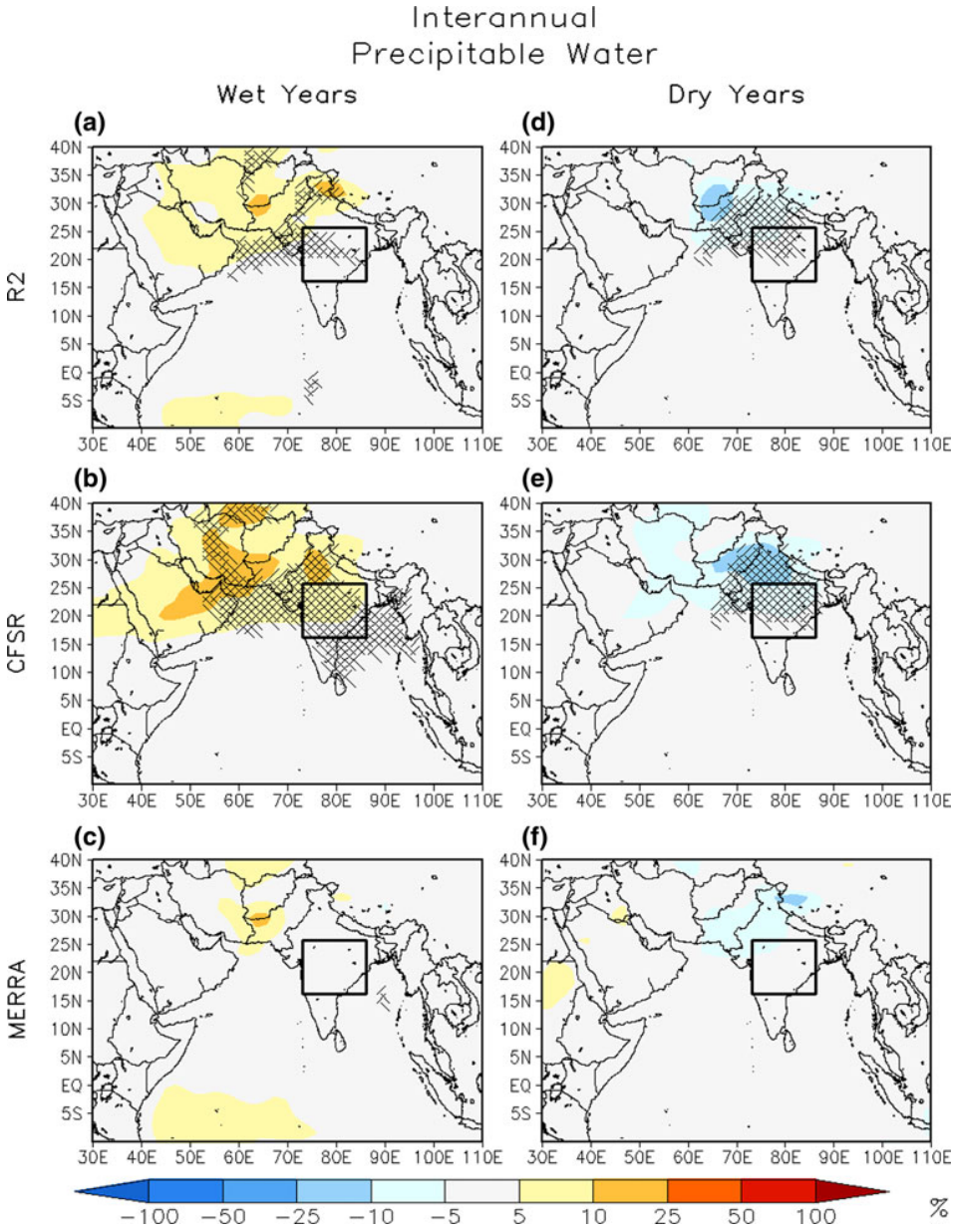


**Fig. 6** Same as Fig. 4, but for PW

We next examine the depiction of the interannual variation of the evaporative sources in the reanalyses. Overall, we observe that during wet (dry) years, evaporative sources of all origin including oceanic and continental are increased (decreased) (Fig. 8). This is to be expected, as increased rainfall totals during wet years must be supplied by increased moisture. For R2, the greatest increase in moisture source in wet years occurs locally over central India and remotely from eastern Africa (Fig. 8a). For CFSR, the largest increase in wet years originates from the remote Arabian Sea and the Bay of Bengal and with moderate local evaporative source from central and southern India (Fig. 8b). For MERRA, the greatest increase in moisture source occurs over central India and far eastern Africa (Fig. 8c). For dry years, R2 receives less moisture from the surrounding tropical waters (Fig. 8d). CFSR displays an overall reduction of moisture over the entire monsoon region (Fig. 8e). Similarly, MERRA shows a reduction in moisture sources, albeit by a smaller amount (Fig. 8f).

The main difference between the reanalyses is in the relative contribution of remote and local evaporative sources in wet and dry years. R2 shows the strongest interannual variation of the local evaporative source over central India, whereas CFSR shows it over the remote oceans.

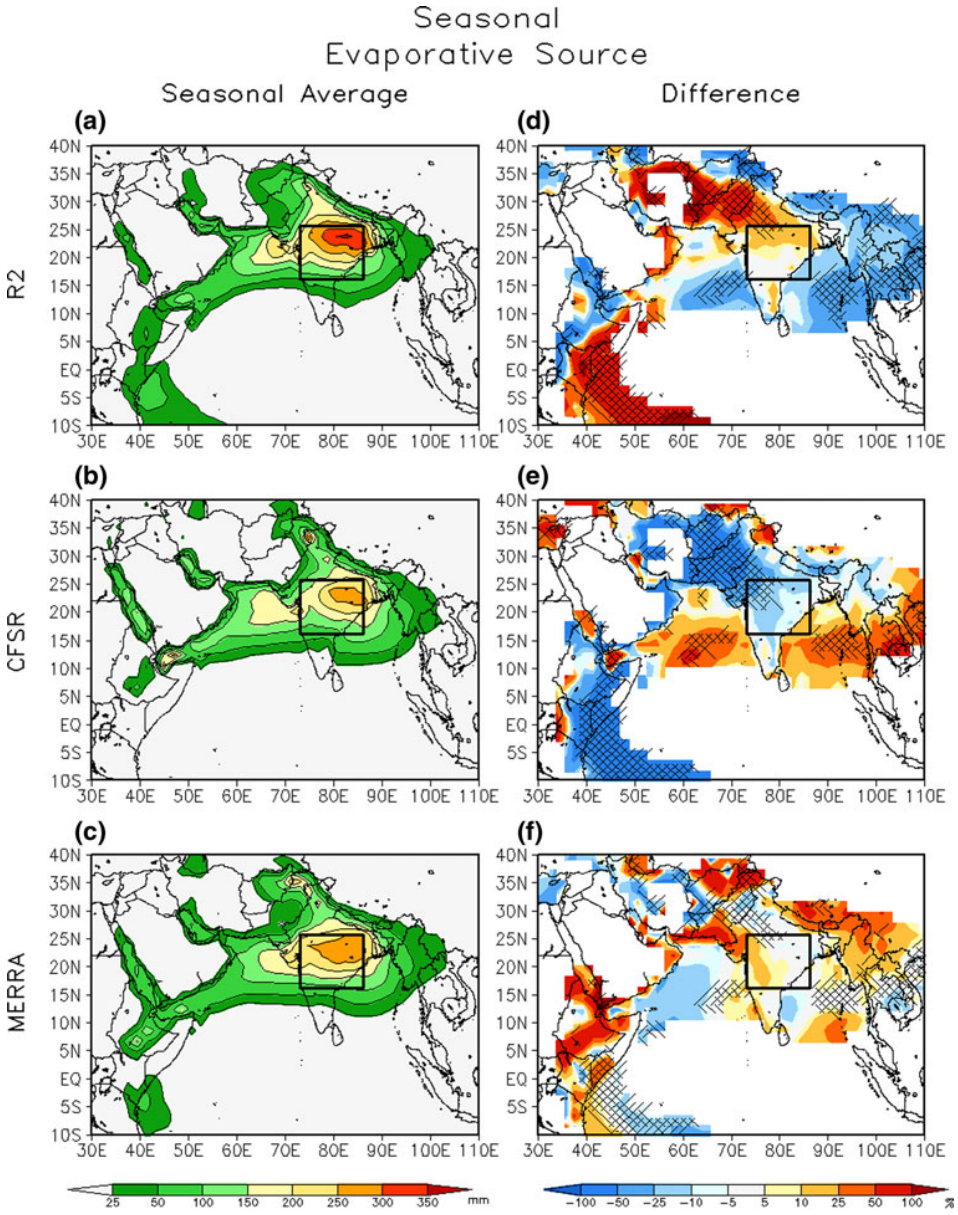


**Fig. 7** Same as Fig. 1, but for evaporative source

4.4 Evaporative source: intraseasonal variability

The differences in location and strength of the evaporative sources for active and break rainfall events during the Indian monsoon from R2 (Fig. 9a, d) and CFSR (Fig. 9b, e) show that active periods feature a significant increase in evaporative source over the northeastern Bay of Bengal, which extends westward over the Arabian Sea. This result is seen in MERRA as well (Fig. 9c). These results are consistent with increased storm activity observed in the Bay of Bengal during the wet spells of the monsoon (Krishnamurthy and Ajayamohan 2010). In the break periods (Fig. 9d–f) there is a corresponding decrease of the evaporative source over most of the domain, especially over the Bay of Bengal.

The evaporation and wind fields respond in the same way to active and break periods as they do to wet and dry years (not shown). The same mechanisms are expected to influence the evaporative sources at this time scale as well.

In this study we attempt to isolate the interannual variability of the intraseasonal variations of the evaporative sources. For this comparison, we examine the intraseasonal anomalies computed from the climatology of each reanalysis separately.

Interestingly, the interannual variability of the intraseasonal variations of the evaporative sources is broadly consistent between the three reanalyses (Figs. 10, 11, 12).

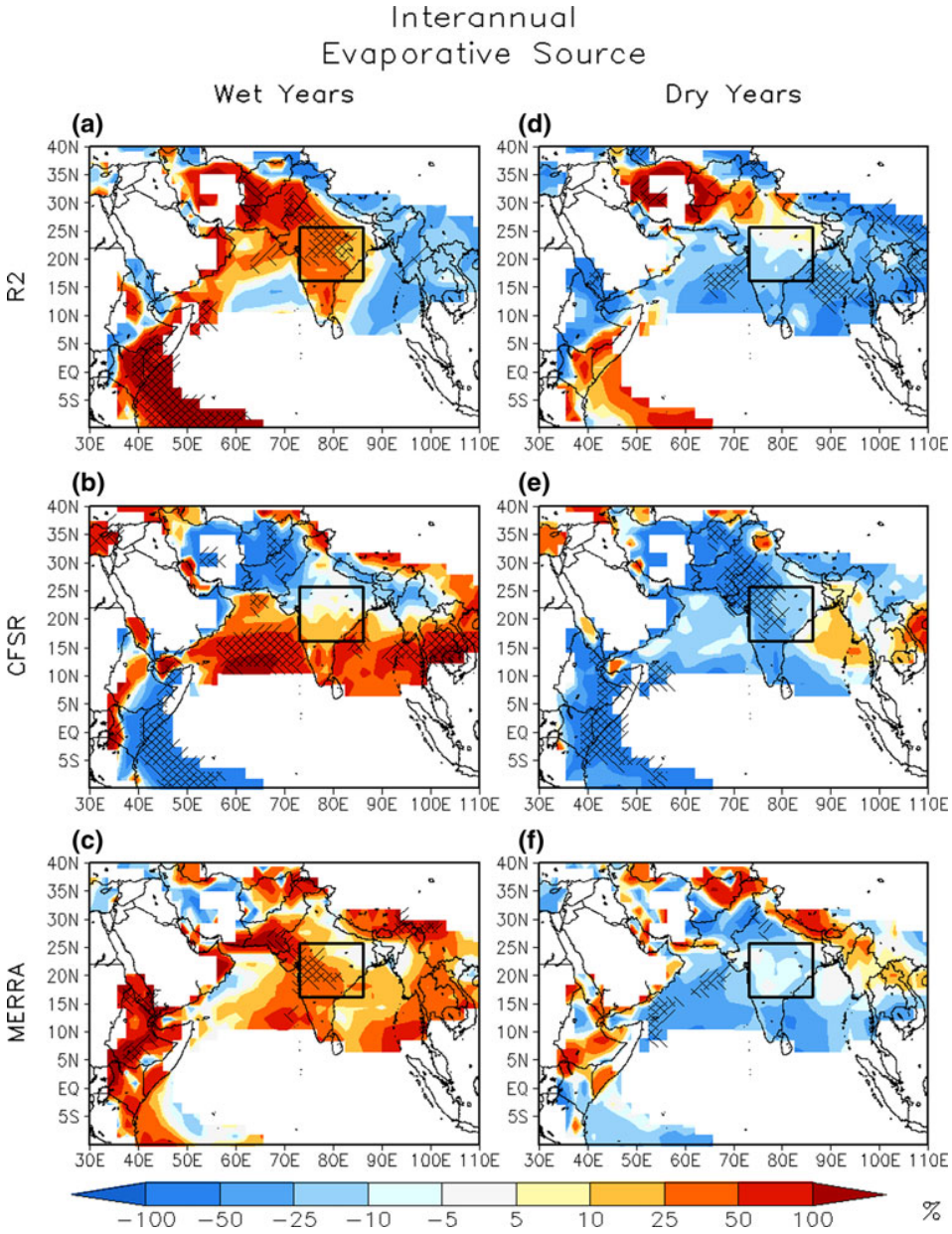


**Fig. 8** Same as Fig. 4, but for evaporative sources for wet and dry years

We observe that there is generally more intraseasonal variability during dry (wet) years, particularly in CFSR (Fig. 11) and more interannual variability in the break (active) periods of the intraseasonal oscillations over central India (the Arabian Sea). The strong interannual variability of the break periods is evident across all reanalyses, but is particularly strong in CFSR.

Given the disparities in the interpretation of the interannual variations of the intraseasonal variability of the Indian Monsoon rainfall (Krishnamurthy and Shukla 2000; Goswami and Ajayamohan 2001) we feel that rainfall may not be necessarily the most appropriate metric to observe the relationship between the seasonal Indian monsoon strength and its intraseasonal activity. This study shows that the relationship is best observed in the evaporative sources of intraseasonal rain events over central India with the break period of the intraseasonal oscillation displaying stronger interannual variations of the evaporative sources. These findings are consistent across the three reanalyses, which differ in the observations they assimilate, the model used for assimilation and the way observations are assimilated. This finding provides a basis for improving the predictability of the intraseasonal variability of the Indian monsoon.

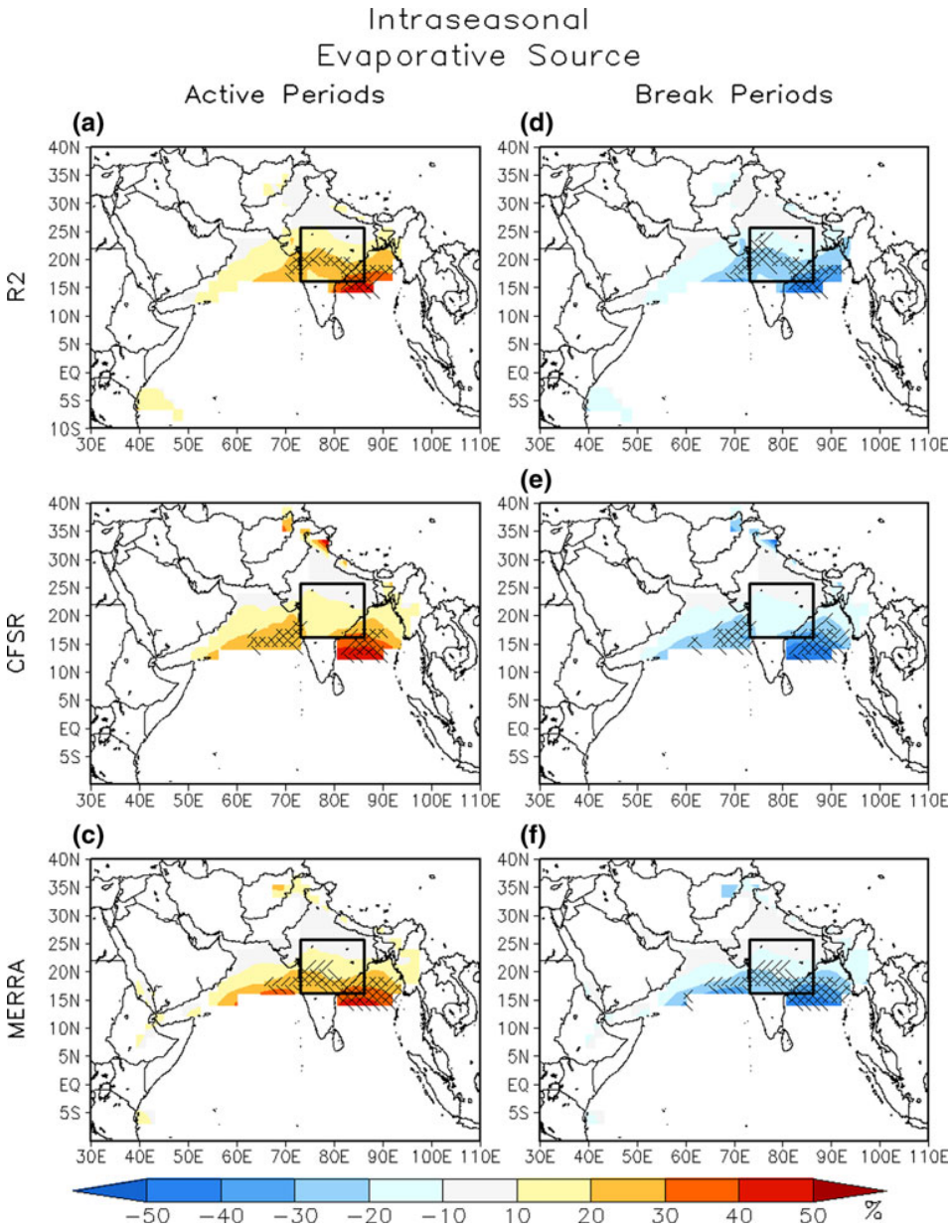


**Fig. 9** Same as Fig. 4, but for evaporative sources in active periods and break periods

## 5 Discussion and conclusions

An intercomparison of the Indian summer monsoon hydroclimate is made between NCEP-DOE (R2; Kanamitsu et al. 2002), CFSR (Saha et al. 2010), and MERRA (Bosilovich et al. 2008). R2 is the oldest of the three reanalyses. Thus far we have seen that the continental parts of the Indian monsoon region exhibit relatively larger differences in the mean and its variability (of the fluxes and PW) between the reanalyses than the oceanic components. We contend that the differences between the LSMs of the reanalyses and the fact that none of the land surface state variables are assimilated as in the case of the atmospheric or oceanic state variables lead to such disparate rendition of the Indian Monsoon hydroclimate. Given that there are significant differences in other parts of the assimilation model of the three reanalyses (Table 1) and they use different assimilation methodologies it is quite difficult to quantitatively attribute the differences between them to a specific physical process. This study therefore highlights the uncertainty in the hydroclimate of the Indian summer monsoon between these reanalyses.

The land–atmosphere interaction is one of the irreconciled parts of the coupled climate system: the impact of

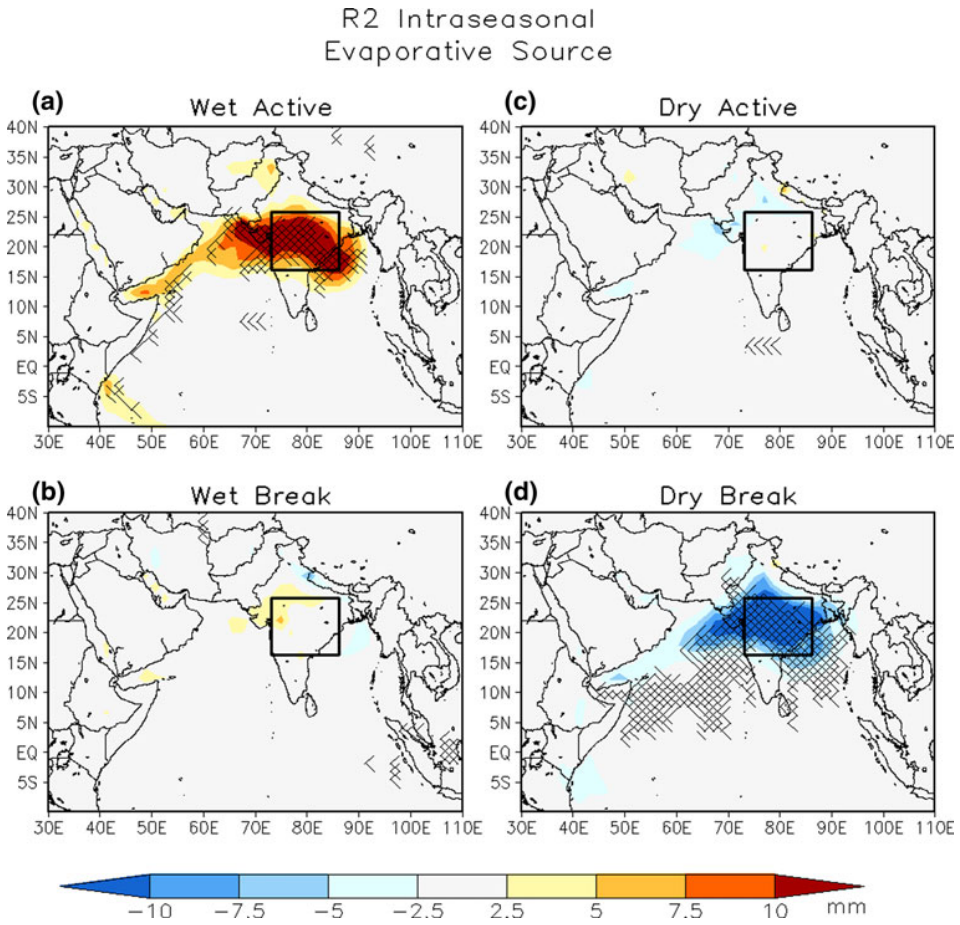


**Fig. 10** Plot showing the evaporative source anomalies for active periods during wet years (**a**), break periods during wet years (**b**), active periods during dry years (**c**), and break periods during dry years (**d**) for R2. These are simple differences from the climatological R2 evaporative source field. Areas of 90% confidence are hatched

precipitation on soil moisture is an obvious feedback but the return path of soil moisture affecting precipitation through modulation of evapotranspiration is one of contention (Koster et al. 2006; Guo et al. 2006). However, the model intercomparison study of Koster et al. (2004) showed that the land–atmosphere coupling strength in the moisture limited regime (Koster et al. 2009) of the central/north Indian region is quite robust. In a moisture limited regime the soil moisture is positively correlated with evaporative flux suggesting that variation of the soil moisture is the controlling factor on the corresponding response of the evaporation (Dirmeyer et al. 2009). In R2 the soil moisture was added to the top soil layer to correct for the unrealistic drying of rain in the monsoonal regions (Kanamitsu et al. 2002). This led to an excessive supply of moisture for local convection (Roads et al. 2002) that led to dessication of the overlying atmospheric column leading to observed predominance of the local evaporative source for central India rain events.

In a more recent study Zhang et al. (2011) indicate that the atmospheric Global Forecast System (GFS; relatively newer version of the atmospheric model from that in Saha et al. 2006)-Noah model exhibits a weak land–atmosphere coupling strength compared to other models in the Global Land–Atmosphere Coupling Experiment (GLACE; Koster et al. 2006). However, they show that when Noah is coupled to another atmospheric model the land–atmosphere coupling strength improves slightly but yet comparatively smaller than other GLACE models. They further find that evapotranspiration in Noah is highly sensitive to soil wetness in the top 10 cm thick soil layer. In any case the absence of using observed rainfall as in R2 and improvements in the parameterization of the fluxes in Noah (as noted in Sect. 2.1) has led to a substantial reduction in the land based evaporative source of the Indian monsoon. For MERRA, Dirmeyer et al. (2011) showed that it displays strong land–atmosphere coupling strength over the Indus valley (which is roughly co-incident with parts of central India and extend further northwest into Pakistan) and moderate coupling strength over rest of central India in the boreal summer season.

It is apparent from our analysis that CFSR has climatologically the least evaporation from the continental regions of the Indian summer monsoon, followed by

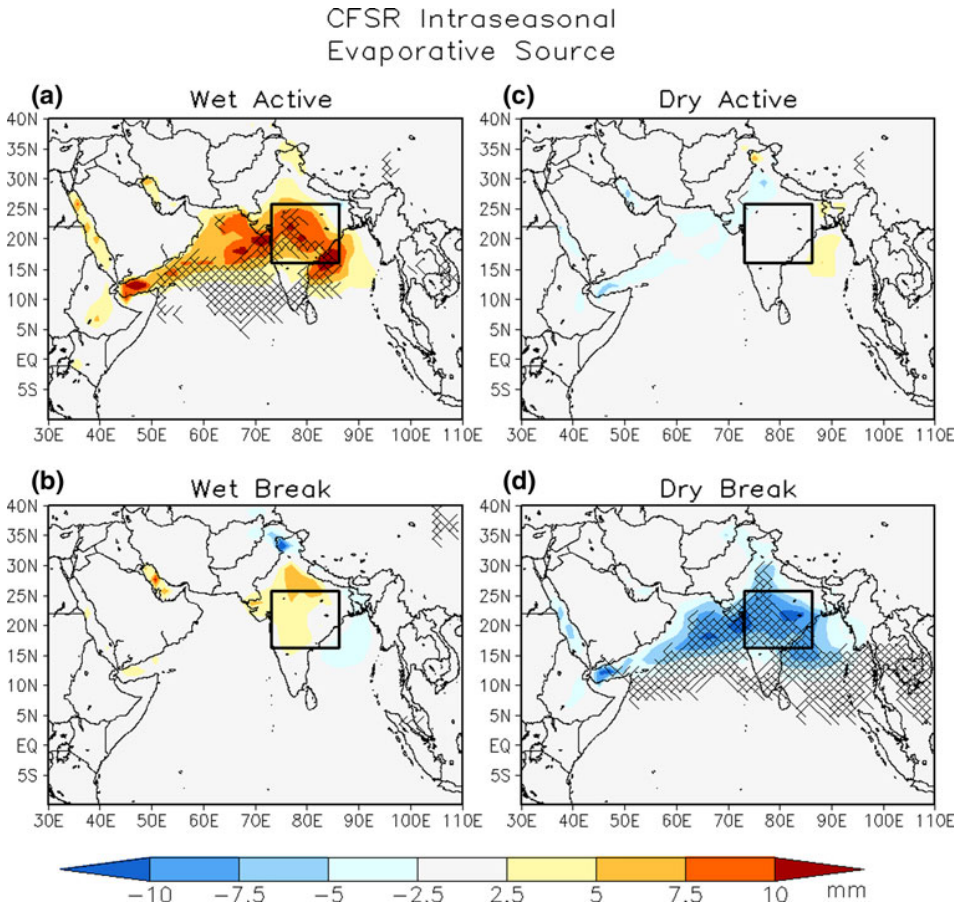


**Fig. 11** Same as Fig. 10, but for CFSR

MERRA and then R2. Comparatively, CFSR shows much higher evaporation rates over the neighboring oceans. Similarly, the 925-hPa westerly winds in the northern Indian Ocean are strongest in R2, whereas they are weakest in CFSR. Furthermore, the precipitable water is climatologically less in R2 over central India than in the other reanalyses. A consequence of these features is that uncertainties in the seasonal mean evaporative source, as calculated by a QIBT, show a more local influence of evaporative sources in R2 and a more remote influence of evaporative sources in CFSR when compared to average analysis.

When we compare the reanalyses on an interannual time scale, we observe that the 925-hPa and PW fields vary the most between reanalyses. In terms of the evaporative sources, R2 (CFSR) showed the largest interannual variations of local (remote oceanic) sources. MERRA showed comparable interannual variations of local (continental) and remote (oceanic) evaporative sources.

An analysis of the intraseasonal differences in evaporative sources indicates that across reanalysis datasets, the Bay of Bengal and areas to the southeast of India have the most influential role in providing moisture for rainfall during active periods. This is most likely associated with the presence of LPSs and tropical cyclones advecting off the water and onto the continental regions during active periods (Krishnamurthy and Ajayamohan 2010). The opposite scenario occurs during dry years in the absence of LPSs.

Finally, we observe that across all reanalyses, there is a distinct interannual signal in the intraseasonal oscillations of the evaporative sources. Our analysis shows that during dry years, ISO activity is enhanced over India. Additionally, break periods show more interannual variability than do active periods. This is a significant result, in the sense that it provides hope for improving intra-seasonal predictability given that there is some evidence for seasonal predictability of the interannual variability of the Indian monsoon (Kang and Shukla 2005; Wang et al. 2005, 2009). It may be noted that the finding of this study has implications for also improving weather prediction by targeting enhanced observations during active phases over Bay of Bengal for improved intial analysis for tropical cyclone genesis forecasts (Zhou et al. 2010; Reale et al. 2009).

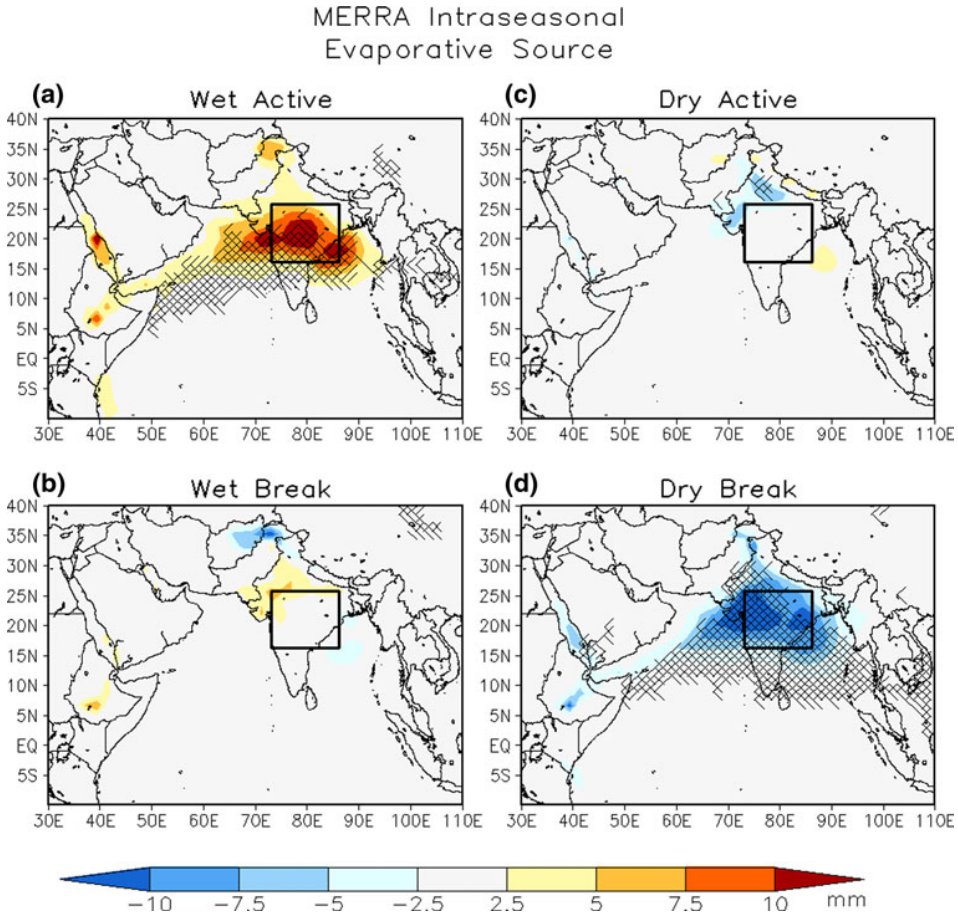


**Fig. 12** Same as Fig. 10 but for MERRA

**Acknowledgments** The authors would like to acknowledge the expert guidance of Kathy Fearon of COAPS for her editorial corrections on an earlier version of the manuscript. We acknowledge the resources of the Computational and Information Systems Laboratory of NCAR to obtain some of the observational datasets used for verification in this study. We also thank Dr. Paul Dirmeyer of Center for Ocean, Land and Atmosphere Studies (COLA) for sharing the Fortran code of the back trajectory program. The useful review comments and suggestions of three anonymous reviewers on an earlier version of the manuscript is also acknowledged. This work is supported by NOAA grant NA070AR4310221 and the USDA.

## References

Wang B et al. (2005) Fundamental challenge in simulation and prediction of summer monsoon rainfall. Geophys Res Lett L15711. doi:10.1029/2005GL022734

Ek MB et al (2003) Implementation of Noah land surface model advances in the National Centers for Environmental Prediction operational mesoscale Eta model. J Geo Res Letters 108:12-1–12-16

Mitchell KE et al (2004) The multi-institution North American Land Data Assimilation System (NLDAS): utilizing multiple GCIP products and partners in a continental distributed hydrological modeling system. J Geophys Res 109:D07S90. doi:10.1029/2003JD003823

Bamzai AS, Shukla J (1999) Relation between Eurasian snow cover, snow depth, and the Indian summer monsoon: an observational study. J Climate 12:3117–3132

Benton GS et al (1950) The role of the atmosphere in the hydrologic cycle. Trans Am Geophsy Union 31:61–73

Betts AK, Chen F, Mitchell KE, Janjic Z (1997) Assessment of the land surface and boundary layer models in the two operational versions of the NCEP Eta model using FIFE data. Mon Weather Rev 125:2896–2916

Bloom S, Takacs L, DaSilva A, Ledvina D (1996) Data assimilation using incremental analysis updates. Mon Wea Rev 124:1256–1271

Bosilovich MG et al (2008) Evaluation of precipitation in reanalyses. J Appl Meteorol Climatol 47:2279–2299

Brubaker KL et al (1993) Estimation of continental precipitation recycling. J Climate 6:1077–1089

Budyko MI (1974) Climate and life. Academic Press, London

Cadet D, Reverdin G (1981) Water vapour transport over the Indian ocean during summer 1975. Tellus 33:476–487

Chan SC, Misra V (2009) A diagnosis of the 1979–2005 extreme rainfall events in the Southeast US with isentropic moisture tracing. Mon Wea Rev 138:1172–1185

Delworth TL, Manabe S (1988) The influence of potential evaporation on the variabilities of simulated soil wetness and climate. J Climate 1:523–547

Delworth TL, Manabe S (1989) The influence of soil wetness on near-surface atmospheric variability. J Climate 2:1447–1462

Derber JD, Parrish DF, Lord SJ (1991) The new global operational analysis system at the National Meteorological Center. Weather Forecast 6:538–547

Dirmeyer PA, Brubaker KL (1999) Contrasting evaporative moisture sources during the drought of 1988 and the flood of 1993. J Geophysical Res 104:19383–19397

Dirmeyer PA, Schlosser CA, Brubaker KL (2009) Precipitation, recycling and land memory: an integrated analysis. J Hydrometeorol 10:278–288. doi:10.1175/2008JHM1016.1

Dirmeyer PA, Schlosser CA, Brubaker KL (2011) The terrestrial segment of soil moisture-climate coupling. Geophys Res Lett L16702, doi:10.1029/2011GL048268

Ek MB, Mahrt L (1991) OSU 1-D PBL model user's guide. Dep. of Atmos. Sci., Oreg. State University, Corvallis, Oregon

Gadgil S (2003) The Indian monsoon and its variability. Annu Rev Earth Planet Sci 31:429–467

Goswami BN, Ajayamohan RS (2001) Intraseasonal oscillations and interannual variability of the Indian monsoon. J Climate 14:1180–1198

Guo Z et al (2006) GLACE: the global land atmosphere coupling experiment. Part II Anal J Hydrometeor 7:611–625

Jones C et al (2004) Climatology of tropical intraseasonal convection anomalies: 1979–2002. J Climate 17:523–539

Joyce RJ et al (2004) CMORPH: a method that produces global precipitation estimates from passive microwave and infrared data at high spatial and temporal resolution. J Hydrometeor 5:487–503

Kanamitsu M et al (2002) NCEP-DOE AMIP-II reanalysis (R-2). Bull Amer Meteor Soc 83:1631–1643

Kang I-S, Shukla J (2005) Dynamical seasonal prediction and predictability of monsoon. In: Wang B (ed) The Asian monsoon. Praxis Publishers Ltd, Chichester, pp 585–612

Kerr JM (1996) Sustainable development of rainfed agriculture in India. EPTD discussion paper no. 20

Kirtman BP, Shukla J (2000) Influence of the Indian summer monsoon on ENSO. Q J R Meteorl Soc 126:213–239

Kleist DT, Parrish DF, Derber JC, Treadon R, Errico RM, Yang R (2009) Improving incremental balance in the GSI 3DVAR analysis system. Mon Wea Rev 137:1046–1060

Koren V, Schaake JC, Mitchell KE, Duan QY, Chen F, Baker J (1999) A parameterization of snowpack and frozen ground intended for NCEP weather and climate models. J Geophys Res 104:19569–19585

Koster RD et al (2000) A catchment-based approach to modeling land surface processes in a general circulation model, 1: model structure. J Geophys Res 105:24809–24822

Koster RD et al (2004) Regions of strong coupling between soil moisture and precipitation. Science 305:1138–1140

Koster RD et al (2006) GLACE: the global land–atmosphere coupling experiment. Part I Overv J Hydrometeor 7:590–610

Koster RD, Guo Z, Dirmeyer PA, Yang R, Mitchell K, Puma MJ (2009) On the nature of soil moisture in land surface models. J Climate 22:4322–4335

Krishnamurthy V, Ajayamohan RS (2010) Composite structure of monsoon low pressure systems and its relation to Indian rainfall. J Clim 23:4285–4305

Krishnamurthy V, Kinter III JL (2003) The Indian monsoon and its relation to global climate variability. In: Rodó X, Comín F (eds) Global Climate: current research and uncertainties in the climate system. Springer, Berlin, pp 186–236

Krishnamurthy V, Kirtman BP (2003) Variability of the Indian ocean: relation to monsoon and ENSO. Quart J Roy Meteor Soc 129:1623–1646

Krishnamurthy V, Kirtman BP (2009) Relation between Indian monsoon variability and SST. J Climate 22:4437–4458

Krishnamurthy V, Shukla J (2000) Intraseasonal and interannual variability of rainfall over India. J Climate 13:4366–4377

Krishnamurthy V, Shukla J (2006) Intraseasonal and seasonally persisting patterns of Indian monsoon rainfall. J Climate 20:3–20

Krishnamurti TN, Subrahmanyam D (1995) The 30–50 day mode at 850 mb during MONEX. J Atmos Sci 39:2088–2095

Kumar K et al (1999) On the weakening relationship between the Indian monsoon and ENSO. Science 284:2156–2159

Kumar SV et al (2008) A land surface data assimilation framework using the land information system: Description and application. Adv Water Resour 31:1419–1432

Lawrence DM, Webster PJ (2001) Interannual variations of the intraseasonal oscillation in the South Asian summer monsoon region. J Climate 14:2910–2922

Lim YK et al (2002) Temporal and spatial evolution of the Asian summer monsoon in the seasonal cycle of synoptic fields. J Climate 15:3630–3644

Meehl GA (1994) Coupled land–ocean–atmosphere processes and south Asian monsoon variability. Science 266:263–267

Meehl GA (1997) The South Asian monsoon and the tropospheric biennial oscillation. J Climate 10:1921–1943

Merrill JT (1989) Atmospheric long-range transport to the Pacific Ocean. Chemical Oceanogr 10:15–50

Misra V (2008) Coupled interactions of the monsoons. Geophys Res Letters 35:L12705

Mooley DA, Parthasarathy B (1984) Fluctuations in All-India summer monsoon rainfall during 1871–1978. Clim Change 6:287–301

Nigam S, Ruiz-Barradas A (2006) Seasonal hydroclimate variability over North America in global and regional reanalyses and AMIP simulations: varied representation. J Climate 15:815–837

Pan HL, Mahrt L (1987) Interaction between soil hydrology and boundary-layer development. Bound-Layer Meteorol 38:185–202

Parrish DF, Derber JC (1992) The National Meteorological Center's spectral statistical interpolation system. Mon Wea Rev 120:1747–1763

Rajeevan M et al (2006) High resolution daily gridded rainfall data for the Indian region: analysis of break and active monsoon spells. Curr Sci 91:296–306

Reale O, Lau WK, Susskind J, Brin E, Liu E, Risshojgaard LP, Fuentes M, Rosenberg R (2009) AIRS impact on the analysis and forecast track of tropical cyclone Nargis in a global data assimilation and forecasting system. Geophys Res Lett 36:L06812. doi:10.1029/2008GL037122

Reynolds RW, Rayner NA, Smith TM, Stokes DC, Wang W (2002) An improved in situ and satellite SST analysis. J Climate 15:1609–1625

Rienecker MM et al (2011) MERRA: NASA's modern-era retrospective analysis for research and applications. J Climate 24:3624–3648

Roads J, Kanamitsu M, Stewart R (2002) CSE water and energy budgets in the NCEP-DOE reanalysis-II. J Hydrometeor 3:227–248

Robock A et al (2003) Evaluation of the North American land data assimilation system over the southern great plains during the warm season. J Geophys Res 108:8846. doi:10.1029/2002JD003245

Ruiz-Barradas A, Nigam S (2004) Warm season rainfall variability over the US great plains in observations, NCEP and ERA-40 reanalyses, and NCAR and NASA atmospheric model simulations. J Climate 18:1808–1830

Saha S et al (2006) The climate forecast system at NCEP. J Clim 19:3483–3517. doi:10.1175/JCLI3812.1

Saha S et al (2010) The NCEP climate forecast reanalysis. Bull Amer Meteor Soc 91:1015–1057

Saji NH et al (1999) A dipole mode in the tropical Indian Ocean. Nature 401:360–363

Shepard D (1968) A two-dimensional interpolation function for irregularly spaced data. Proceedings of the 1968 23rd ACM National Conference 517–524

Singh SV et al (1992) Interannual variability of the Madden-Julian Oscillations in Indian summer monsoon rainfall. J Climate 5:973–978

Trenberth KE, Guillemot CJ (1998) Evaluation of the atmospheric moisture and hydrological cycle in the NCEP/NCAR reanalyses. Climate Dyn 14:213–231

Trenberth KE, Dai A, Rasmussen RM, Parsons DB (1999) Atmospheric moisture recycling: role of advection and local evaporation. J Climate 12:1368–1381

Trenberth KE, Dai A, Rasmussen RM, Parsons DB (2003) The changing character of precipitation. Bull Amer Soc 84:1205–1217

Wang B, Lee J-Y et al. (2009) Advance and prospect of seasonal prediction: Assessment of the APCC/CliPAS 14-model ensemble retrospective seasonal prediction (1980–2004). Clim Dyn 33. doi:10.1007/s00382-008-0460-0

Wang B et al (2001) Interannual variability of the Asian summer monsoon: contrasts between the Indian and the western North Pacific-East Asian monsoons. J Climate 14:4073–4090

Zhang L, Dirmeyer PA, Wei J, Guo Z, Lu C-H (2011) Land-atmosphere coupling strength in the global forecast system. J Hydromet 12:147–156

Zhou Y, Lau WK, Reale O, Rosenberg R (2010) AIRS impact on precipitation analysis and forecast of tropical cyclones in a global data assimilation and forecasting system. Geophys Res Lett 37:L02806. doi:10.102/2009GL041494